Talanta 94 (2012) 184–188

Contents lists available at SciVerse ScienceDirect

Talanta

journal homepage: www.elsevier.com/locate/talanta

Halogen-free ionic liquid as an additive in zinc(II)-selective electrode: Surface analyses as correlated to the membrane activity

Maryam F. Al-Asousi[a], Adel F. Shoukry[b,*], Abdul Hadi Bu-Olayan[b]

[a] Family Sciences Department, College for Women, Kuwait University, P.O. Box 5969, Safat 13060, Kuwait
[b] Chemistry Department, Faculty of Science, Kuwait University, P.O. Box 5969, Safat 13060, Kuwait

ARTICLE INFO

Article history:
Received 25 January 2012
Received in revised form 4 March 2012
Accepted 6 March 2012
Available online 12 March 2012

Keywords:
Zn(II) ion-selective electrode
Halogen-free ionic liquid
X-ray photoelectron spectroscopy
Ion-scattering spectroscopy
Atomic force microscopy

ABSTRACT

Two conventional Zn(II) polyvinyl chloride (PVC) membrane electrodes have been prepared and characterized. They were based on dibenzo-24-crown-8 (DBC) as a neutral carrier, dioctyl phthalate (DOP) as a plasticizer, and potassium tetrakis (p-chlorophenyl) borate, KTpClPB or the halogen-free ionic liquid, tetraoctylammonium dodecylbenzene sulfonate [TOA][DBS] as an additive. The use of ionic liquid has been found to enhance the selectivity of the sensor. For each electrode, the surfaces of two membranes were investigated using X-ray photoelectron, ion-scattering spectroscopy and atomic force microscopy. One of the two membranes was conditioned by soaking it for 24 h in a 1.0×10^{-3} M $Zn(NO_3)_2$ solution and the second was soaked in bi-distilled water for the same interval (24 h). Comparing the two surfaces indicated the following: (a) the high selectivity in case of using [TOA][DBS] as an additive is due to the extra mediation caused by the ionic liquid and (b) the working mechanism of the electrode is based on phase equilibrium at the surface of the membrane associated with ion transport through the bulk of the membrane.

1. Introduction

Zinc ion is an important divalent cation in biological systems; it influences DNA synthesis, microtubule polymerization, gene expression, apoptosis, immune system function, and the activity of enzymes such as carbonic anhydrase and matrix metalloproteinase [1]. Moreover, chelatable Zn(II) ions are present at especially high concentrations in the brain [2], pancreas [3], and spermatozoa [4].

Several techniques have been reported for the determination of zinc(II) cation including flame atomic absorption spectrometry [5], fluorometry [6], UV–visible spectrophotometry [7], inductively-coupled plasma atomic emission spectrometry [8], potentiometry [9–21], and voltammetry [22]. Among these techniques, potentiometry using ion-selective electrodes is relatively simple, fast, accurate and inexpensive; further, it is applicable to both in-field and in-line analyses.

With the discovery of crown ethers, the focus on complexation through covalent interactions shifted to that of non-covalent interactions. The later suits the establishment of phase equilibrium systems; therefore, many ion selective electrodes for various cations have been developed based on crown ethers and their derivatives as neutral carriers [23–26]. The function of a crown ether as an electro-active material for ion-selective electrodes is based on such diverse parameters as the structure and cavity size of the cyclic ether, the stability and selectivity of its metal ion complex, and the solubility and ability of the crown ether to extract the metal ion into the membrane phase. Dibenzo-24-crown-8 (DBC) has been used previously as a neutral carrier for Zn(II) plastic membrane ion selective electrodes containing sodium tetraphenyl borate (NaTPB) as an additive [27]. The electrode exhibited Nernstian response to Zn(II); however, its selectivity was relatively poor towards many divalent cations.

Room-temperature ionic liquids are a novel class of salts that, in recent years, have engaged exponential attention as green chemicals. Imidazolium (C_4mim)-based ILs with tetrafluoroborate (BF_4^-) and hexafluorophosphate (PF_6^-) anions have, so far, been the focus of numerous applications including their use in ion selective electrodes [28,29]. Nevertheless, the classification of these compounds as green chemicals has not taken into account their entire life cycle. The fluorine-based anions of these ILs have been the subject of extensive debates about the possible eventual decomposition, under certain circumstances, into the toxic hydrofluoric acid [30]. Further, studies using single-crystal X-ray diffraction [31] proved the formation of 1-butyl-3-methylimidazolium fluoride monohydrate complex, $[C_4mim]F{\cdot}H_2O$, during the preparation and drying of $[C_4mim][PF_6]$. It has also been reported [32] that in drastic acid medium, $[PF_6]^-$ may be converted to $[PO_4]^{3-}$.

* Corresponding author. Tel.: +965 24987374; fax: +965 24816482.
E-mail addresses: M.alasousi@ku.edu.kw (M.F. Al-Asousi), adelshoukry@gmail.com, a.shoukry@ku.edu.kw (A.F. Shoukry), buolayan@yahoo.com (A.H. Bu-Olayan).

0039-9140/$ – see front matter © 2012 Elsevier B.V. All rights reserved.
doi:10.1016/j.talanta.2012.03.016

This raised the importance of the use of halogen-free ionic liquid as a truly green chemical for different applications including ion-selective electrodes. In this paper a halogen-free ionic liquid is used as an additive to enhance the selectivity of the electrode. Moreover, the electrode surface was analysed by X-ray photoelectron and ion-scattering spectroscopy, and atomic force microscopy to throw light to the working mechanism of the electrode.

2. Experimental

2.1. Reagents and materials

All reagents used were of analytical grade and doubly-distilled water was used throughout. Tetraoctylammonium bromide (TOAB) (Sigma–Aldrich), sodium dodecylbenzene sulfonate (NaDBS) (Sigma–Aldrich), dibenzo-24-crown-8 (DBC) (Sigma–Aldrich), polyvinyl chloride (PVC) of high molecular weight (Fluka), dioctyl phthalate (DOP) 99% (Sigma–Aldrich), potassium tetrakis (p-chlorophenyl) borate, KTpClPB (Sigma–Aldrich), tetrahydrofuran (Fluka), lead(II) nitrate (Sigma–Aldrich), and potassium nitrate (Sigma–Aldrich) were used. The method of synthesis of the ionic liquid, tetraoctylammonium-dodecylbenzene sulfonate [TOA][DBS] was similar to that described elsewhere [33]. Briefly, equimolar amounts of TOAB and NaDBS were mixed in a 1:1 water–acetone solvent. The mixture was stirred, while heated until the acetone evaporated completely. The mixture was then separated into an oil and aqueous phase. The mixture was transferred to a separating funnel and the aqueous phase was removed. The resultant crude [TOA][DBS] oil was purified by shaking with water several times. The ionic liquid was then dried with anhydrous sodium sulfate.

2.2. Construction of the electrode

The membrane was prepared by dissolving appropriate amounts of PVC, DOP, carrier DBC, and KTpClPB or [TOA][DBS] in about 25 ml of tetrahydrofuran. The solution was poured into a 10 cm diameter glass Petri dish and left to dry overnight. A 10 mm diameter disc was cut out from the prepared membrane and glued to the polished end of a PVC cap attached to a glass tube. The electrode body was filled with a solution that is 1.0×10^{-1} M in NaCl and 1.0×10^{-3} M in $Zn(NO_3)_2$, in which the tip of a Ag/AgCl wire was immersed.

2.3. Measurement and electrochemical system

The measurements were carried out with an Orion, model 420A pH/mV meter. A caron circulator thermostat was used to control the temperature of the test solution. The following electrochemical system was used:

$$Ag|AgCl|KCl_{sat}||Pb^{2+}\text{testsolution}|\text{membrane}|NaCl\,10^{-1}\text{ M} + Zn(II)\,10^{-3}\text{ M}|AgCl|Ag$$

2.4. The calibration curve

Suitable increments of the standard $Zn(NO_3)_2$ solution were added to 50 ml of bi-distilled water in which the prepared sensor and the reference electrode were immersed and the e.m.f. value obtained for each addition was recorded at 25 °C.

2.5. Effect of foreign ions

The selectivity coefficients of the Zn(II) electrode were determined by the matched potential method (MPM) [34].

2.6. X-ray photoelectron spectroscopy

Spectra were recorded on a Thermo ESCALAB 250 Xi using mono-chromatized Al Kα radiation (1486.6 eV) with a spot size of 320 μm. Spectra acquisition and processing employed Thermo Avantage Version 4.58 software. For each experiment, the plastic membrane of the electrode was carefully removed, placed in the preparation chamber (via the sample holder), and degassed until about a 10^{-6} mBar vacuum was obtained. It was then transferred into the analysis chamber where a vacuum was maintained at 10^{-9}–10^{-10} mBar. The analyses were performed using the following parameters: pass energy = 20 eV, Dwell time = 50 ms, and step size = 0.1 eV. A flood gun was used in standard charge compensation mode to neutralize the charge build-up on the surface of insulating samples. Depth profiling was accomplished using an argon ion gun with a 2 kV energy source and 2 μA current. Etching times of 0, 30, and 60 s were applied. Surface images were obtained using the following parameters: CAE = 80 eV, step = 0.250 eV, and scan amplitude = 950.08 eV.

2.7. Ion scattering spectroscopy

An Escalab model 250 Xi probe system was used. The incident ions were He^+ with a primary beam energy of about 1000 eV and a scattering angle (Θ) of 130°. From a gold standard, the primary beam energy E_o was determined as 910 eV.

2.8. Atomic force microscopy

Atomic force measurements were obtained using a scanning probe microscope (model RTESP, from Veeco Instruments, USA), provided with tapping mode tips. Elasticity measurements were obtained with a phosphorus-doped Si tip (pyramidal shape) using a tip curvature radius of 3.5–4.5 μm, a spring constant of 20–80 N/m, and a resonant frequency nominal of 278–311 KHz (Nano Devices, Veeco Metrology, Santa Barbra, California). The lateral scan range was 115–135 μm, pertaining to 30–40 μm z-scans.

3. Results and discussion

3.1. Composition of the membranes

The electrode was made from a membrane containing 64.08, 32.08, 3.2, and 0.64% (w/w) of PVC, DOP, DBC, and KTpClPB or [TOA][DBS], respectively. DBC was chosen as neutral carrier because its cavity size (1.05 Å) is well suited for the uptake of zinc ion (ionic radius 0.88 Å) [27]. When using KTpClPB as an additive, the calibration curve slope was 29.2 mV/pZn over a concentration range of 1.7×10^{-5} to 1.3×10^{-2} M with a detection limit of 0.87 μg Zn(II)/mL. The latter was estimated according to IUPAC recommendation [33]. The practical response time of the electrode was always ≤15 s. When using [TOA][DBS] as an additive, a calibration graph slope of 31.4 mV/pZn was obtained over a concentration range of 3.4×10^{-5} to 3.8×10^{-2} M with a detection limit of 1.53 μg Zn(II)/mL.

3.2. Effect of pH

The stability of sensor's potential reading was investigated over the acidic pH range in order to determine the working pH range of the electrode. The pH value of the test solution, 1.0×10^{-3} M $Zn(NO_3)_2$, was adjusted with solutions of HNO_3 and NaOH (0.1–1.0 M). No significant variation of the potential reading was observed within the average pH range of 4.6–6.5 in both cases of using KTpClPB or [TOA][DBS] as an additive. In this range, the

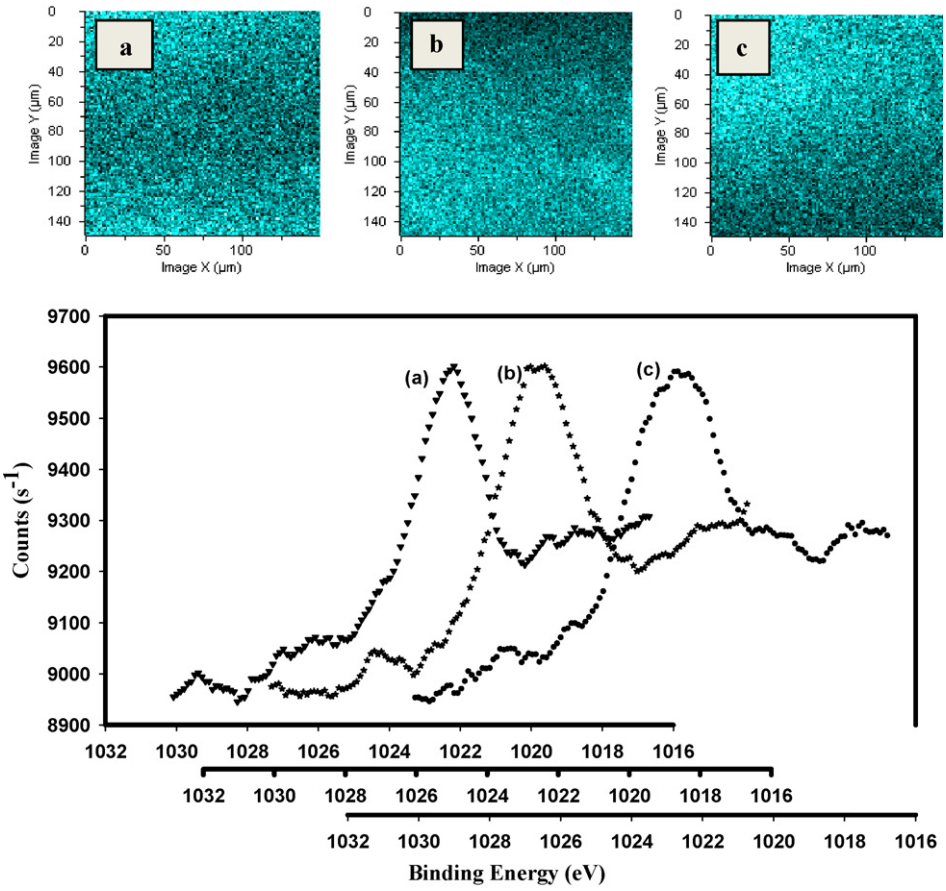

Fig. 1. X-ray photoelectron images and spectra of Zn 2p core electrons: (a) at the surface of the membrane, (b) after etching for 30 s, and (c) after etching for 60 s.

electrode can be safely used for Zn(II) determination without using pH buffering solutions.

3.3. Interference of foreign ions

The matched potential method, proposed in 1984 by Gadzekpo and Christian [34] and recommended in 1995 by IUPAC [35], was applied to determine the selectivity coefficient values of the electrodes (Table 1). Comparing to both the separate solution and fixed interference methods [36], this technique has the advantage of being independent of Nickolsky–Eisenman equation. So, Nernstian portions of the response of the primary and interfering ions are not required.

Both investigated electrodes showed higher selectivity than that of an electrode containing NaTPB as an additive (Table 1) [27]. This is probably due to the greater lipophilicity of KTpClPB and [TOA][DBS] compared to NaTPB. Moreover, the ionic liquids have proved ability to extract Zn(II) from the aqueous solution into the membrane side [37], thus increasing the rate of formation of the ionophore at both the internal and external gel layers of the membrane. This also explains the better selectivity of [TOA][DBS] versus KTpClPB.

Table 1
Selectivity coefficients K^{pot}_{Zn,Jz^+} of Zn(II)-selective electrode.

Ion	K^{pot}_{Zn,Jz^+} [a]	K^{pot}_{Zn,Jz^+} [b]	K^{pot}_{Zn,Jz^+} [c]
Na^+	1.6×10^{-2}	1.2×10^{-2}	3.0×10^{-1}
K^+	8.8×10^{-3}	1.1×10^{-3}	1.7×10^{-1}
Ag^+	1.8×10^{-2}	1.1×10^{-1}	2.0×10^{-1}
Mg^{2+}	3.5×10^{-2}	5.8×10^{-3}	2.0×10^{-1}
Ca^{2+}	2.4×10^{-2}	6.8×10^{-3}	1.5×10^{-1}
Ba^{2+}	2.4×10^{-1}	3.0×10^{-3}	1.0×10^{-1}
Co^{2+}	5.8×10^{-2}	4.9×10^{-3}	1.0×10^{-1}
Ni^{2+}	2.7×10^{-2}	3.9×10^{-3}	–
Cu^{2+}	8.4×10^{-3}	2.0×10^{-3}	2.0×10^{-1}
Pb^{2+}	3.4×10^{-2}	5.2×10^{-3}	1.3×10^{-1}
Cd^{2+}	1.8×10^{-2}	6.5×10^{-3}	3.5×10^{-1}
Hg^{2+}	1.1×10^{-2}	1.4×10^{-2}	1.3×10^{-1}
Al^{3+}	2.1×10^{-2}	2.0×10^{-2}	1.9×10^{-1}
Fe^{3+}	4.2×10^{-1}	2.2×10^{-2}	1.6×10^{-1}

[a] Using membrane containing KpClPB as the additive.
[b] Using membrane containing [TOA][DBS] as the additive.
[c] Literature values (MPM) [27].

3.4. X-ray photoelectron spectroscopy of Zn 2p core electrons

In this technique, the spectrum is a combination of an overall trend due to resonance structures that derive from core electronic states of the elements under analysis, transmission characteristics of the spectrometer, and the energy loss process within the sample. The resonance (intrinsic) peaks together with the background features of the spectrum offer information about the chemical composition of the sample (electrode's membrane) surface.

The high resolution Zn 2p spectrum, in addition to the corresponding chemical image of the surface, of conditioned membranes containing KTpClPB as additive at different depths are shown in Fig. 1a. The spectrum and image were scanned again after sputtering the surface with a 2 keV beam of argon ions for 30 and 60 s (Fig. 1b and c). All spectra are characterized with a Zn $2p_{3/2}$ peak at about 1022 eV with almost the same counts/second. This indicates the transport mechanism of the electrode's response. This is confirmed by comparing chemical images (b) and (c) with image (a).

Table 2
Roughness parameters of Zn(II)-responsive membranes as determined by atomic force microscopy.

Membrane's additive	Soaking medium	RMS[a] (nm)	Ra[b] (nm)	Rq[c] (nm)	Rmax[d] (nm)
KTpClPB	Distilled water	12.7	0.803	0.989	0.363
	1.0×10^{-3} M Zn(II) solution	38.6	1.34	2.36	2.45
[TOA][DBS]	Distilled water	26.2	1.04	1.04	0.460
	1.0×10^{-3} M Zn(II) solution	146	11.7	19.8	2.89

[a] Root mean square.
[b] Roughness average.
[c] Root mean roughness.
[d] The maximum roughness depth.

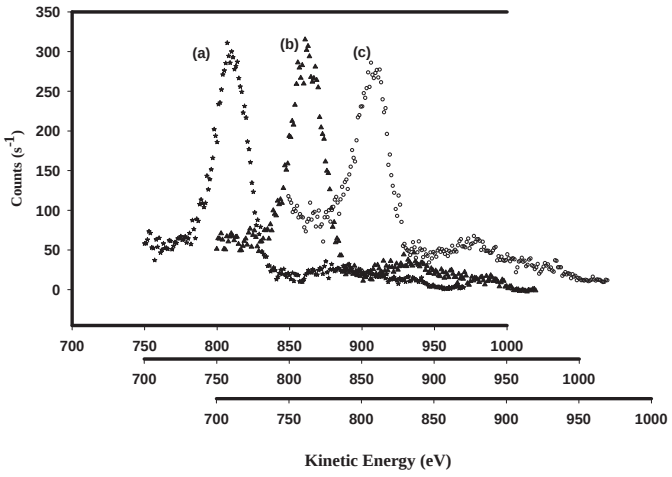

Fig. 2. Ion scattering spectra of Ar ions back-scattered from surface Zn(II) at the surface of the membrane (a), after etching for 30 s (b), and after etching for 60 s (c).

Similar results were obtained for membranes containing the ionic liquid as an additive.

3.5. Ion scattering spectroscopy

The ion scattering spectroscopy (ISS) involved firing a beam of mono-energetic He ions at the surface of the electrode and measuring the kinetic energies of the ions that were scattered back. The ISS spectrum (Fig. 2) is obtained by recording the number of scattered ions collected per second as a function of their kinetic energy. The technique is uniquely sensitive to the outermost layer of the surface. In the present study, the analysis was accomplished at different depths inside a conditioned membrane containing KTpClPB (Fig. 2). The results revealed the existence of Zn(II) inside the bulk of the membrane. This confirms the ionic transport of the primary ion during the conditioning process of the electrode.

3.6. Atomic force microscopy

Atomic force microscopy (AFM) is a direct descendant of scanning tunneling microscopy. The cause for its design was the desire to use scanning probe microscopy on poorly conductive materials. For electron microscopy techniques, the low density and insulating nature of most polymers dictate that the sample must be treated prior to image acquisition. Commonly, this necessitates the exposure of the polymeric sample to a vacuum environment. With the AFM, the sample can be imaged in its natural state; hence the potential incidence of sample preparation induced artifacts is reduced. Moreover, AFM can measure, in numerical values, the roughness of the surface.

3.6.1. Atomic force microscopy of membrane containing KTpClPB

Membranes containing KTpClPB, as an additive, was conditioned by soaking them in 1.0×10^{-3} M $Zn(NO_3)_2$ solution for 24 h. For comparison, another membrane was soaked in distilled water for the same period, 24 h. The AFM images of the two membranes are shown in (Fig. 3a and b) and their roughness parameters are given in Table 2. The results indicate that the surface of the membrane soaked in Zn(II) solution is more rough than that of the membrane soaked in water (Table 2). This distinct difference in the morphology

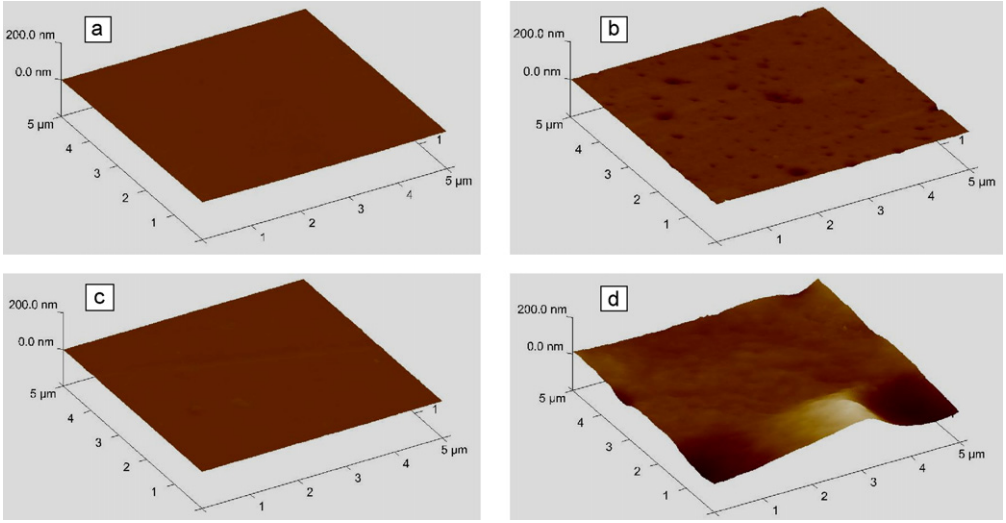

Fig. 3. 3D AFM (5 µm × 5 µm × 200 nm) images of Zn(II)-responsive membranes containing KTpClPB (a and b) or [TOA][DBS] (c and d) as additive. (a and c) Membranes soaked in bidistilled water for 24 h. (b and d) Membranes soaked in 1.0×10^{-3} M Zn(II) solution for 24 h.

of the two surfaces is most plausibly due to the complexation of Zn(II) with DBC at the surface of the membrane.

3.6.2. Atomic force microscopy of membrane containing [TOA][DBS]

Fig. 3c and d shows the AFM images of the surfaces of two membranes containing [TOA][DBS] as an additive. The image in (c) is of a membrane soaked for 24 h in bi-distilled water while that in (d) is a membrane soaked for 24 h in 1.0×10^{-3} M $Zn(NO_3)_2$ solution. Comparing Fig. 3c with Fig. 3d, it is evident that the surface of the membrane soaked in Zn(II) solution is rougher than that of the membrane soaked in water. This is confirmed by the results of roughness parameters given in Table 2. The cause of this difference in the morphology of the two membranes is the formation of Zn(II)–DBC complex in the gel layer covering the membrane surface.

It is evident that the surface of the membrane containing the ionic liquid is, in general, rougher than the membrane containing KpClPB (Table 2). This is likely due to the oily nature of the ionic liquid, which adds to the plasticization of the membrane.

4. Conclusion

A highly selective plastic membrane Zn(II)-ion selective electrode can be constructed based on dibenzo-24-crown-8 as a neutral carrier and KTpClPB or the halogen-free ionic liquid [TOA][DBS] as an additive. The electrode containing [TOA][DBS] exhibited higher selectivity for Zn(II) than the electrode containing KTpClPB. Comparative surface analyses of membranes soaked in Zn(II) solution and in distilled water indicated that the origin of the electrode potential is a phase boundary exchange equilibrium at the interfacial junction separating the membrane from the test solution. This equilibrium is associated with ion transport through the membrane. The atomic force microscopy revealed that the formation of an ion-ionophore complex during the conditioning process of the electrode substantially changes the morphology of the membrane's surface.

Acknowledgements

The supports of the University of Kuwait received through the College of Graduate Studies, the facilities of ANALAB (grant no. GS 02/08), SAF (grant no. GS 03/01), the X-ray Photoelectron Spectroscopy Unit, and the Nanoscopy Science Center are gratefully acknowledged.

References

[1] J.M. Berg, Y. Shi, Science 271 (1996) 1081–1085.
[2] C.J. Frederickson, Int. Rev. Neurobiol. 31 (1989) 145–238.
[3] P.D. Zalewski, S.H. Millard, I.J. Forbes, O. Kapaniris, A. Slavotinek, W.H. Betts, A.D. Ward, S.F. Lincoln, I. Mahadevan, J. Histochem. Cystochem. 42 (1994) 877–884.
[4] P.D. Zalewski, X. Jian, L.L.L. Soon, W.G. Breed, R.F. Seamark, S.F. Lincolin, A.D. Ward, F.Z. Sun, Reprod. Fertil. Dev. 8 (1996) 1097–1105.
[5] Q. Li, X.H. Zhao, Q.Z. Lv, G.G. Liu, Sep. Purif. Technol. 55 (2007) 76–81.
[6] M. Hosseini, Z. Vaezi, M.R. Ganjali, F. Faridbod, S. Dehghan Abkenar, K. Alizadeh, M. Salavati-Niasari, Spectrochim. Acta A 75 (2010) 978–982.
[7] P. Kaur, S. Kaur, A. Mahajan, K. Singh, Inorg. Chem. Commun. 11 (2008) 626–629.
[8] P. Wilhartitz, S. Dreer, R. Krismer, O. Bobleter, Mikrochim. Acta 125 (1997) 45–52.
[9] N.R. Gupta, S. Mittal, S. Kumar, S.K.A. Kumar, Mater. Sci. Eng. C 28 (2008) 1025–1030.
[10] R. Kojuma, S. Kamata, Anal. Sci. 10 (1994) 409–412.
[11] M. Shamsipur, S. Rouhani, M.R. Ganjali, H. Sharghi, H. Eshghi, Sens. Actuators B 59 (1999) 30–34.
[12] A. Bhatola, B.K. Puri, Talanta 49 (1999) 485–493.
[13] P.C. Pandey, G. Dingh, Sens. Actuators B 85 (2002) 256–262.
[14] V.K. Gupta, A. Kumar, R. Mangla, Sens. Actuators B 76 (2001) 617–623.
[15] A.R. Fakhari, M. Shamsipur, Kh. Ghanbari, Anal. Chim. Acta 460 (2002) 177–183.
[16] M.B. Gholivand, Y. Mozaffari, Talanta 59 (2003) 399–407.
[17] V.K. Gupta, A.K. Jain, R. Mangla, P. Kumar, Electroanalysis 13 (12) (2001) 1036–1040.
[18] V.K. Gupta, A.K. Jain, G. Maheswari, Chem. Anal. (Warsaw) 51 (2006) 889–897.
[19] V.K. Gupta, S. Agarwal, A. Jakob, H. Lang, Sens. Actuators B 114 (2006) 812–818.
[20] M. Hosseini, S. Dehghan Abkenar, M.R. Ganjali, F. Faridbod, Mater. Sci. Eng. C 31 (2011) 428–433.
[21] P. Singh, A.K. Singh, A.K. Jain, Electrochim. Acta 56 (2011) 5386–5395.
[22] X. Lu, Z. Wang, Z. Geng, J. Kang, J. Gao, Talanta 52 (2000) 411–416.
[23] A.N. Haoyun, W.U. Yangjie, Z. Zhijun, J. Inclusion Phenom. Mol. Recognit. Chem. 11 (1991) 303–311.
[24] V.K. Gupta, P. Kumar, Anal. Chim. Acta 389 (1999) 205–212.
[25] S.K. Mittal, S.K. Ashok Kumar, H.K. Sharma, E-J. Chem. 7 (3) (2010) 849–855.
[26] S. Yajima, T. Nakajima, M. Higashi, K. Kimura, Chem. Commun. 46 (2010) 1914–1916.
[27] V.K. Gupta, M. Al Khayat, A.K. Minocha, P. Kumar, Anal. Chim. Acta 532 (2005) 153–158.
[28] A. Safavi, N. Maleki, F. Honarasa, F. Tajabadi, F. Sedaghatpour, Electroanalysis 19 (2007) 582–586.
[29] B. Peng, J. Zhu, X. Liu, Y. Qin, Sens. Actuators B: Chem. 133 (2008) 308–314.
[30] M.G. Freire, C.M.S.S. Neves, I.M. Marrucho, J.A.P. Coutinho, A.M. Fernandes, J. Phys. Chem. A 114 (2010) 3744–3749.
[31] R.P. Swatloski, J.D. Holbrey, R.D. Rogers, Green Chem. 5 (2003) 361–366.
[32] A.E. Visser, R.P. Swatloski, W.M. Reichert, S.T. Griffin, R.D. Rogers, Ind. Eng. Chem. Res. 39 (2000) 3596–3604.
[33] T. Tsukatani, H. Katano, H. Tatsumi, M. Deguchi, N. Hirayama, Anal. Sci. 22 (2006) 199–200.
[34] V.P.Y. Gadzekpo, G.D. Christian, Anal. Chim. Acta 164 (1984) 279.
[35] Y. Umezawa, K. Umezawa, H. Sato, Pure Appl. Chem. 67 (1995) 507.
[36] Y. Umezawa, P.B. Hlmann, K. Umezawa, K. Tohda, S. Amemiya, Pure Appl. Chem. 72 (10) (2000) 1851–2082.
[37] A.P. de los Ríos, F.J. Hernández-Fernández, S. Sánchez-Segado, L.J. Lozano, J.I. Moreno, C. Godínez, Chem. Eng. Trans. 21 (2010) 625–630.